

CP violation and mass hierarchy at medium baselines in the large θ_{13} era

S. Dusini^a, A. Longhin^b, M. Mezzetto^a, L. Patrizii^c, M. Sioli^{c,d}, G. Sirri^c, F. Terranova^{e,f}

^a Istituto Nazionale di Fisica Nucleare, Sez. di Padova, Padova, Italy

^b Laboratori Nazionali di Frascati dell'INFN, Frascati (Rome), Italy

^c Istituto Nazionale di Fisica Nucleare, Sez. di Bologna, Bologna, Italy

^d Dep. of Physics, Univ. di Bologna Bologna, Italy

^e Dep. of Physics, Univ. di Milano-Bicocca, Milano, Italy

^f Istituto Nazionale di Fisica Nucleare, Sez. di Milano-Bicocca, Milano, Italy

Abstract

The large value of θ_{13} recently measured by reactor and accelerator experiments opens unprecedented opportunities for precision oscillation physics. In this paper, we reconsider the physics reach of medium baseline superbeams. For $\theta_{13} \simeq 9^\circ$ we show that facilities at medium baselines – i.e. $L \simeq \mathcal{O}(1000\text{km})$ – remain optimal for the study of CP violation in the leptonic sector, although their ultimate precision strongly depends on experimental systematics. This is demonstrated in particular for facilities of practical interest in Europe: a CERN to Gran Sasso and CERN to Phyäsalmi ν_μ beam based on the present SPS and on new high power 50 GeV proton driver. Due to the large value of θ_{13} , spectral information can be employed at medium baselines to resolve the sign ambiguity and determine the neutrino mass hierarchy. However, longer baselines, where matter effects dominate the $\nu_\mu \rightarrow \nu_e$ transition, can achieve much stronger sensitivity to $\text{sign}(\Delta m^2)$ even at moderate exposures.

1 Introduction

After an experimental search lasted more than a decade [1, 2, 3, 4], we know quite precisely the size of the mixing angle between the first and third neutrino family (θ_{13}) [5, 6, 7, 8]. Such value turned out to be extremely large - in fact, very close to previous limits set by CHOOZ [9] and Palo Verde [10]. A large value of θ_{13} not only constraints models for neutrino mass and mixing [11] but, even more, opens up the possibility to perform precision physics in the leptonic sector with artificial neutrino beams in a way that resembles what was done for quark mixing in the B-factory era [12]. In the past, several experimental strategies have been considered [13, 14], corresponding to possible values of θ_{13} . The most extreme, addressing $\sin^2 2\theta_{13}$ as small as 10^{-4} , required novel acceleration techniques to achieve unprecedented neutrino beam intensities and purity. The results from T2K, Daya-Bay, RENO and Double-Chooz allow to reconsider these scenarios, seeking for less challenging experimental setups to establish CP violation in the leptonic sector and determine the neutrino mass pattern (“mass hierarchy”). The experimental proposals will take advantage of the large $\nu_\mu \rightarrow \nu_e$ oscillation probability due to $\theta_{13} = 8.9^\circ \pm 0.4^\circ$ [15], likely relieving the constraints on the detector mass and accelerator power. In this paper we address some of these issues, firstly on general ground and, then, driven by practical considerations. On general ground we discuss to what extent the constraints on beam power, purity and systematic uncertainty can limit our capability to establish CP violation in the leptonic sector using Superbeams [16, 17, 18, 19, 20, 21]. We consider the optimal baseline to search for CP violation at the atmospheric scale, i.e. a medium baseline ($L \simeq 1000$ km) with neutrino energies of $E \simeq 1$ GeV and a far detector capable of reconstructing quasi-elastic, deep-inelastic and resonance final states (liquid argon TPC). It is well known that such baseline represents a poor choice for the simultaneous determination of CP violation (CPV) and mass hierarchy, which could be better achieved with longer baselines and wide-band neutrino beams [22, 23]. Hence, in the context of medium baselines we evaluate the deterioration of the sensitivity on CPV due to the ignorance on the neutrino mass hierarchy. Similarly, we compare the CP reach of the facility when the far detector is located at a baseline

optimal for the determination of mass hierarchy through the exploitation of matter effects ($L \gg 1000$ km). The results of such general study are relevant in setting experimental issues and to establish a European strategy for precision measurements in the large θ_{13} era.

First, we discuss to what extent the Gran Sasso underground Laboratories could be considered as a viable candidate to host the facility for CP violation. As an alternative option [24], we detail the physics reach of a new shallow depth laboratory able to host significantly larger detector masses than what can be accommodated in the present experimental halls of LNGS. Finally, we compare the CP reach of these facilities with a multipurpose detector [25, 26] located at longer baselines, i.e. from ~ 1000 up to 2290 km (CERN-to-Phyäsalmi [27, 28, 29, 30]), in order to establish to what extent the choice of a baseline better suited for the mass hierarchy can affect the CP reach. All comparisons are done as a function of the intensity of the neutrino source, detector mass and systematic uncertainties. When needed, beam parameters are re-optimized ab initio (i.e. at the target-horn level) to achieve best performance for a given configuration and allow a fair comparison among various options.

2 Facilities at medium baselines

All current long-baseline experiments are in the medium baseline range (~ 1000 km) either because they are tuned to be at the peak of the oscillation probability at the atmospheric scale (MINOS: 730 km, T2K: 293 km, NOVA: 810 km) or because they maximize the event rate for $\nu_\mu \rightarrow \nu_\tau$ transitions (OPERA: 730 km). At these baselines, matter density can be safely considered constant and $\nu_\mu \rightarrow \nu_e$ transition probabilities are commonly expressed by a perturbative expansion on $\sin 2\theta_{13}$ and $\alpha \equiv \Delta m_{21}^2/\Delta m_{31}^2$. In the following, $P(\nu_\mu \rightarrow \nu_e)$ is approximated as [31]:

$$\begin{aligned}
P(\nu_\mu \rightarrow \nu_e) &\simeq \sin^2 2\theta_{13} \sin^2 \theta_{23} \frac{\sin^2[(1 - \hat{A})\Delta]}{(1 - \hat{A})^2} \\
&- \alpha \sin 2\theta_{13} \xi \sin \delta \sin(\Delta) \frac{\sin(\hat{A}\Delta)}{\hat{A}} \frac{\sin[(1 - \hat{A})\Delta]}{(1 - \hat{A})} \\
&+ \alpha \sin 2\theta_{13} \xi \cos \delta \cos(\Delta) \frac{\sin(\hat{A}\Delta)}{\hat{A}} \frac{\sin[(1 - \hat{A})\Delta]}{(1 - \hat{A})} \\
&+ \alpha^2 \cos^2 \theta_{23} \sin^2 2\theta_{12} \frac{\sin^2(\hat{A}\Delta)}{\hat{A}^2} \\
&\equiv O_1 + O_2(\delta) + O_3(\delta) + O_4 .
\end{aligned} \tag{1}$$

In this formula $\Delta \equiv \Delta m_{31}^2 L/(4E)$ and the terms contributing to the Jarlskog invariant are split into the small parameter $\sin 2\theta_{13}$, the $\mathcal{O}(1)$ term $\xi \equiv \cos \theta_{13} \sin 2\theta_{12} \sin 2\theta_{23}$ and the CP term $\sin \delta$; $\hat{A} \equiv 2\sqrt{2}G_F n_e E/\Delta m_{31}^2$ with G_F the Fermi coupling constant and n_e the electron density in matter. Note that the sign of \hat{A} depends on the sign of Δm_{31}^2 which is positive (negative) for normal (inverted) hierarchy of neutrino masses.

The large size of θ_{13} changes the phenomenology of the medium baseline. In the past it was commonly believed $\sin 2\theta_{13}$ to be at most of the size of α , i.e. a large suppression of the first term in Eq.1 was expected. We know now that $\sin 2\theta_{13}$ overwhelms α by one order of magnitude (~ 0.3 versus ~ 0.03), which makes the determination of the CP-blind term O_1 crucial for precision oscillation physics. Since O_1 is large and depends on the mass hierarchy through \hat{A} , the ignorance on the sign of Δm_{31}^2 plays a role even at medium baselines.

For sake of illustration, Fig. 1 shows the oscillation probability $\mathcal{P}(\nu_\mu \rightarrow \nu_e)$ versus neutrino energy for different choices of the mass hierarchy and the δ_{CP} phase for a baseline of 730 km and $\sin^2 2\theta_{13} = 0.092$. It is evident that effects ruled by the mass hierarchy (matter effects) and the CP phase are of comparable size. At first order they introduce a change in the normalization so that the control of systematic errors becomes crucial. The second oscillation maximum, that can be used to disentangle CP and matter effects, appears at an energy of about 500 MeV. The full exploitation of spectral information down to a few hundreds of MeV points toward a detector

with high granularity, energy resolution and efficiency for low-energy electron neutrinos. That justifies the consensus on the use of liquid argon (LAR) detectors as far detectors for precision experiments at medium baselines (see Sec. 3).

In the following, three configurations will be detailed. All of them exploit a neutrino beam from CERN to the Gran Sasso area and are based on a

1. on-axis detector inside the existing underground laboratory (up to 10 kt mass) (ONA)
2. 7 km off-axis detector (up to 100 kt mass) located in a new shallow depth site (OA7)
3. as above but at 10 km off-axis (OA10)

In particular, OA7 has been studied in the past [24] for the measurement of θ_{13} although the mean neutrino energy is quite far from the oscillation peak; on the other hand, the spectrum of OA10 better matches the region of interest for CP violation at the price of reduced statistics. The first option (ONA) is clearly of great practical interest since it is completely based on existing underground facilities. However, the limited size of the LNGS halls strongly constrains the maximum detector weight [32]. The ICARUS T600 module [33, 34], which is currently in data taking in the Hall B of LNGS (110 m in length), has a dimension of $3.9 \times 4.3 \times 19.6$ m³, corresponding to a liquid argon mass of 0.735 kt (0.476 kt fiducial). The ICARUS T1200 module [35] proposed in 2001 for the CNGS was based on a tank of $10.3 \times 10.3 \times 21$ m³, totaling 1.47 kt (0.952 kt fiducial). Assuming an array of four T1200 modules located in Hall B would allow the installation of a 4 kt fiducial mass detector at Gran Sasso. In addition, a novel design recently considered by the ICARUS Collaboration can increase the total available mass in Hall B up to 7.5 kt [36]. In conclusion, even assuming the availability of extra space at LNGS, the Gran Sasso laboratories could not host a detector with mass larger than 10 kton. In this study 10 kton is considered the largest exploitable mass for the ONA option.

Similarly, two classes of options have been considered for the neutrino source (see Sec. 3). The former, which is based on the existing CERN-SPS, employs at most facilities that are already available; the second one, which considers a new CERN-based proton driver at 50 GeV, allows for higher flexibility in the choice of the beam configuration and better performance on a longer timescale.

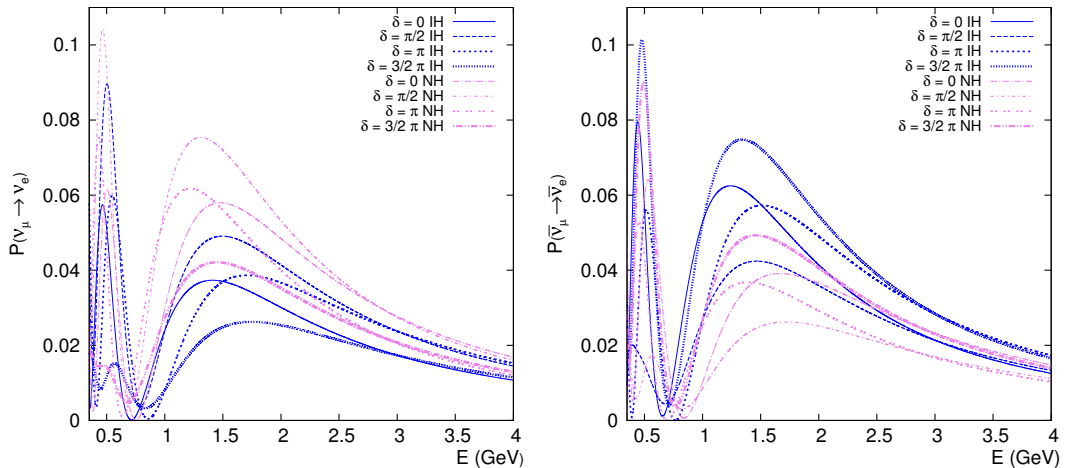


Figure 1: $\mathcal{P}(\nu_\mu \rightarrow \nu_e)$ (left) and $\mathcal{P}(\bar{\nu}_\mu \rightarrow \bar{\nu}_e)$ (right) vs neutrino energy for different choices of the mass hierarchy and δ for a 730 km baseline and $\sin^2 2\theta_{13} = 0.092$.

3 Beamline and detector simulation

The beam parameter optimization for a novel 50 GeV proton driver is based on the results obtained in [37] in the framework of the LAGUNA design study. The most relevant parameters

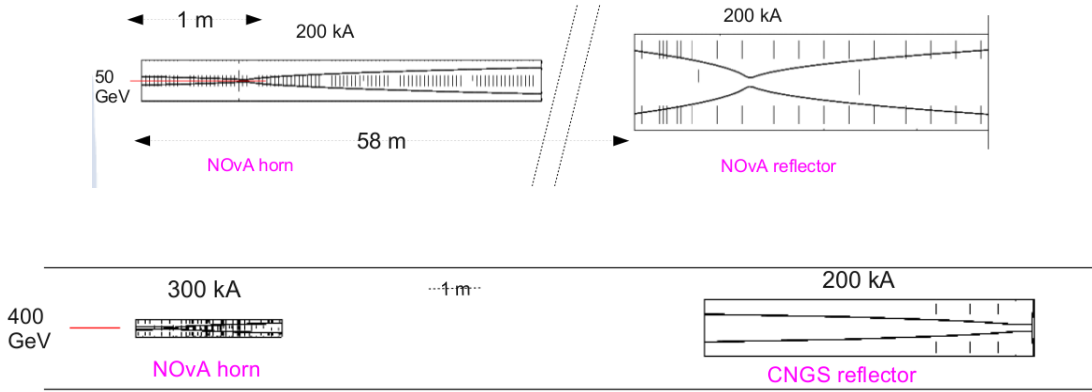


Figure 2: Focusing optics for the 50 (top) and 400 GeV (bottom) proton energy beamline.

are the distances among the target, the upstream focusing horn and the downstream focusing horn (“reflector”), the target length and the length and width of the decay tunnel. Following the approach of Ref. [37], the parameters, together with the geometry of the horn and reflectors were optimized using the sensitivity to θ_{13} as a figure of merit, instead of resorting to intermediate observables as e.g. the number of unoscillated neutrinos. This optimization is also appropriate for the CP reach, especially if the detector technology allows the exploitation of spectral information. The optimal configuration for a ~ 700 km baseline (CERN-to-Gran Sasso) is shown in the top drawing of Fig. 2. The decay tunnel is 90 m long and the optimal radius is 2.2 m. The target consists of a 1 m long graphite rod. Primary interactions in the target were simulated with the GEANT4 [38] QGSP hadronic package and secondaries were traced down to the decay tunnel. The θ_{13} sensitivity was computed using the GLOBES 3.1.11 package [39, 40] and assuming 100 kton LAr far detector (see below).

The neutrino beam from the existing SPS required a dedicated optimization since the current CNGS configuration (on-axis, $\langle E_\nu \rangle \sim 17$ GeV) is not appropriate for CP violation studies. An approach similar to the optimization of the 50 GeV driver was followed. A pre-scan of the beam parameters was carried out using a fast simulation based on the BMPT parameterization [41]. This approach is particularly rewarding since the BMPT formulas are mostly based on data collected with 400 GeV/c and 450 GeV/c protons at CERN-SPS. However, fluxes in the proximity of the optimal parameters were fully simulated with GEANT4. The optimised configuration is shown in the bottom drawing of Fig. 2. The tunnel geometry is the one of CNGS with a length of 1000 m and a radius of 1.225 m. A 1 m long graphite target was used. The corresponding off-axis event rates in the optimal configuration are shown in Fig. 3 together with the rates for the ONA configuration (“50 GeV ON”). All rates are normalized to the proton energy.

The advantage of a dedicated proton driver at 50 GeV is quite evident since the region where most of the CP related information reside is located below 2.5 GeV. Moreover, at these baselines the second oscillation maximum is inaccessible for any configuration based on a 400 GeV accelerator. Similar considerations hold for a low energy (10 GeV optics) re-optimization of CNGS (“CNGS LE on-ax” in Fig. 3), as the one considered in Ref. [42].

Liquid Argon detectors are the most promising technology to address precision oscillation physics. The main advantages of a LAr TPC in ν_e appearance are very high efficiency both for quasi-elastic (80%) and deep-inelastic (90%) interactions combined with a superior NC rejection power. In the following, we considered a contamination of NC due to $\pi \rightarrow e$ misidentification not exceeding 0.1% of the ν_μ CC rate. In the occurrence of QE interaction, the neutrino energy can be fully reconstructed by the lepton energy and direction, since the direction of the incoming neutrino is known in advance. LAr detectors [33, 34, 43] are capable to reconstruct E_ν with a resolution mostly dominated by the electron energy resolution: $\sigma_{E_\nu}/E_\nu \simeq 0.05/\sqrt{E_\nu}$, E_ν being expressed in GeV. On the other hand, energy resolution for DIS- ν_e interaction is driven by the resolution on the hadronic system. In LAr, the latter amounts to $\sigma_{E_h}/E_h \simeq 0.2/\sqrt{E_h(\text{GeV})}$.

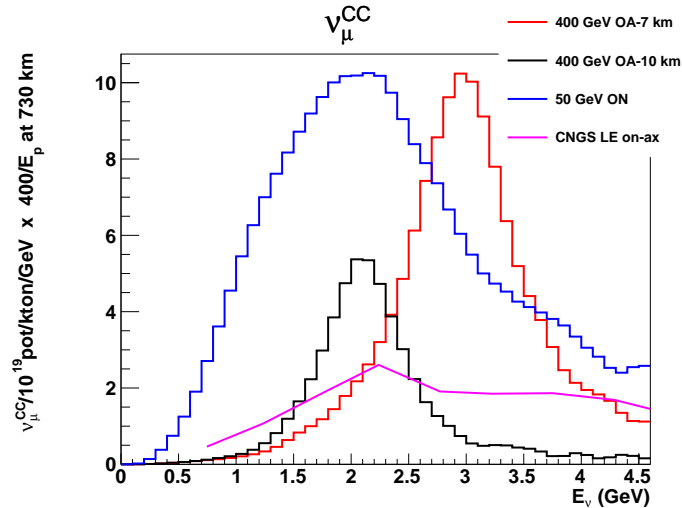


Figure 3: ν_μ^{CC} event rates for the two off-axis (OA) options considered in the text (“400 GeV OA 7-km” and “400 GeV OA 10-km”) and for a dedicated on-axis 50 GeV proton driver (“50 GeV ON”). “CNGS LE on-ax” refers to the low-energy (10 GeV optics) re-optimization of CNGS considered in [42].

In this study, the energy resolution and efficiency for ν_e and $\bar{\nu}_e$ were implemented smearing the final state momenta of the electrons and hadrons. Interactions were simulated using the GENIE Monte Carlo generator [44] and the corresponding migration matrices were implemented in the detector description of GLoBES. The smearing matrices were calculated for ν_e and $\bar{\nu}_e$ separately. They are shown for ν_e events in Fig. 4 (left). In the simulation, a 50 MeV bin width was used. Similarly, the efficiency as a function of energy is shown in Fig. 4 (right).

4 Results

As mentioned above, three possible options were considered in this study: an on-axis detector with limited fiducial mass (ONA), a 7 km (OA7) and 10 km (OA10) off-axis setup leveraging the existing 400 GeV accelerator. In Fig. 5 the ν_e^{CC} appearance spectra convoluted with detector effects for the ONA, OA7 and OA10 options are shown. For the on-axis option, a 50 GeV proton driver with a 10 kt detector was assumed. The power of the proton driver corresponds to $3 \cdot 10^{21}$ pot/y (2.4 MW). For the off-axis options, a 20 kton detector and $1.2 \cdot 10^{20}$ pot/y (0.77 MW) was considered. Clearly, for the 400 GeV proton driver option the power of the driver is constrained by the limitations of the SPS-based neutrino beam, while for the 50 GeV facility, a dedicated multi-MW machine can be envisioned.

The performance of the different options were compared defining as figure of merit the CP violation discovery potential at 3σ . Following [13, 45], we define the “CP coverage” at 3σ as the fraction of possible (true) values of the CP phase δ where the CP conserving hypothesis ($\delta = 0, \pi$) has a p-value smaller than 0.0027. It corresponds to $\chi_{min} > 9$ for $\delta = 0, \pi$ (1 d.o.f.). In each case, we considered separately the possibility that the mass hierarchy is known by the time the facility starts data taking. If the mass hierarchy is not known, the p-value of the null hypothesis is computed as the χ_{min} of the following combinations: ($\delta = 0, \Delta m_{32}^2 > 0$), ($\delta = \pi, \Delta m_{32}^2 > 0$), ($\delta = 0, \Delta m_{32}^2 < 0$), ($\delta = \pi, \Delta m_{32}^2 < 0$).

The 3σ CP coverage in the on-axis facility based on the 50 GeV proton driver is shown in Fig. 6 for 5 years of running with ν and 5 years with $\bar{\nu}$. The corresponding results are shown in Figs. 7 and 8 for the 7 and 10 km off-axis configurations based on the 400 GeV proton driver. In each plot we consider normal and inverted hierarchy, assuming this information to be available or not (color codes) at time of running. The assumed systematic error on flux normalization

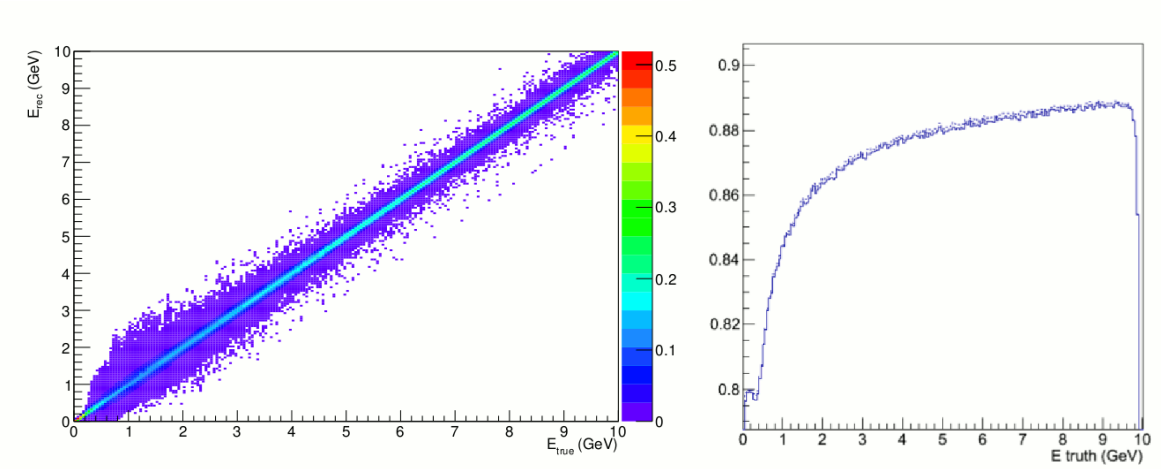


Figure 4: Smearing matrix (left) and efficiency (right) for ν_e CC events.

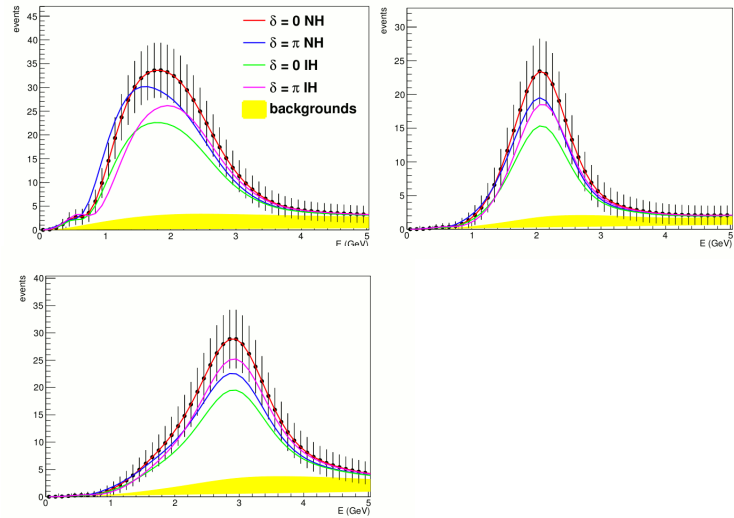


Figure 5: ν_e appearance signal at 730 km for 5 years of data taking, $\sin^2 2\theta_{13} = 0.092$, and normal hierarchy. Upper Left: ONA option, $10 \text{ kt} \otimes 3 \cdot 10^{21} \text{ pot/y}$ (2.4 MW). Upper Right: OA10 option, $20 \text{ kt} \otimes 1.2 \cdot 10^{20} \text{ pot/y}$ (0.77 MW). Lower Left: OA7 option, $20 \text{ kt} \otimes 1.2 \cdot 10^{20} \text{ pot/y}$ (0.77 MW).

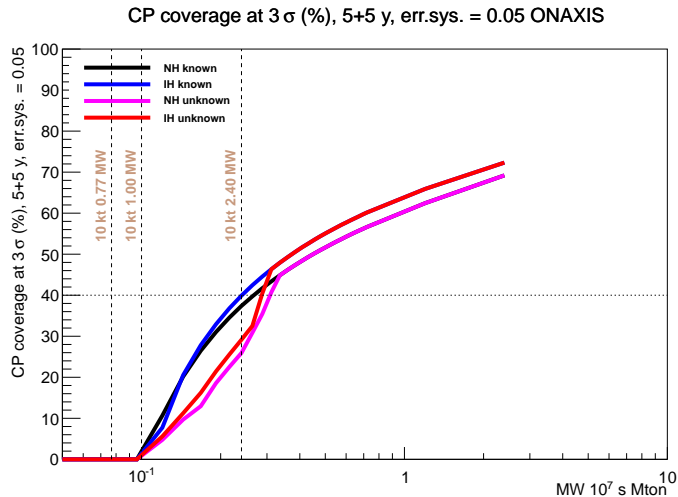


Figure 6: CP coverage at 3σ for 5 years of ν and 5 years of $\bar{\nu}$ running with the on-axis configuration, a 50 GeV proton driver and a systematic error on flux normalization of 5%. We consider normal and inverted hierarchy assuming this information to be either available or not (color codes).

amounts to 5 %.

A comparison of the three options in the case of normal hierarchy (assumed to be unknown) is plotted in Fig. 9.

Some interesting considerations hold either when the results are considered on general ground for any medium baseline facility or when specific CERN-based facilities are envisioned. Firstly, it is clear that the limitation due to the sign degeneracy [46, 47], i.e. the deterioration of the CPV coverage due to the ignorance of the mass hierarchy plays a major role only for limited exposures or detector mass and it is not an intrinsic limitation of medium baselines for such high values of θ_{13} . Large exposures, however, are mandatory to exploit spectral information and thus to remove the sign ambiguity at $L \simeq 730$ km.

The constraints on the minimum exposure is particularly severe when we consider realistic CERN-based facilities. In the vertical lines of Figs. 6 we indicated the CP coverages of a facility whose far detector is hosted in the underground halls of LNGS (maximum LAr mass: 10 kton). It is apparent that LNGS is not appropriate as a far detector site unless a dedicated proton driver well exceeding 2 MW power can be built at CERN. Similar considerations hold for the off-axis facilities that leverage the infrastructure on which the CNGS is built (Fig.7,8). In this case, a new shallow laboratory can overcome the limitation on the detector mass but the low power of the driver constraints the CP coverage well below 50%. Again, the limited statistics reduce the resolution power of spectral information to lift the sign ambiguity, so that prior knowledge of the mass hierarchy increases the CP coverage up to a factor 2.

At large exposures the coverage quickly saturates at $\sim 70\%$ (see Fig.9). This is an intrinsic feature of Superbeams for large θ_{13} where the CP reach is dominated by the systematics on the flux normalization. That is shown in Fig. 10, where systematics are varied from 1% to 10%. In this range, the coverage at saturation decreases from 86% to 60%. This result confirms the key role played by the near detector and by the knowledge of the cross sections and detector efficiency when performing precision physics with Superbeams [48]. In fact, a control of the systematics at the few-percent level remains very challenging, being still at the level of 10.3% for T2K. Clearly, this issue makes the construction of a near detector mandatory for CPV searches. This is particularly relevant for CERN-based facilities, where the installation of a near detector poses additional difficulties from the point of view of engineering and civil infrastructure.

Finally, it is interesting to compare the CP reach of medium baselines with facilities that exploit longer distances to establish the mass hierarchy through the observation of matter effects.

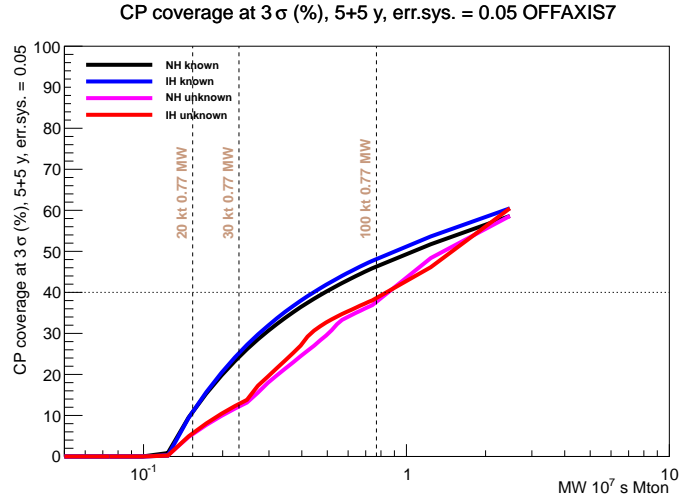


Figure 7: CP coverage at 3σ for 5 years of ν and 5 years of $\bar{\nu}$ running with the off-axis 7 km configuration, a 400 GeV proton driver and a systematic error on flux normalization of 5%. We consider normal and inverted hierarchy assuming this information to be either available or not (color codes).

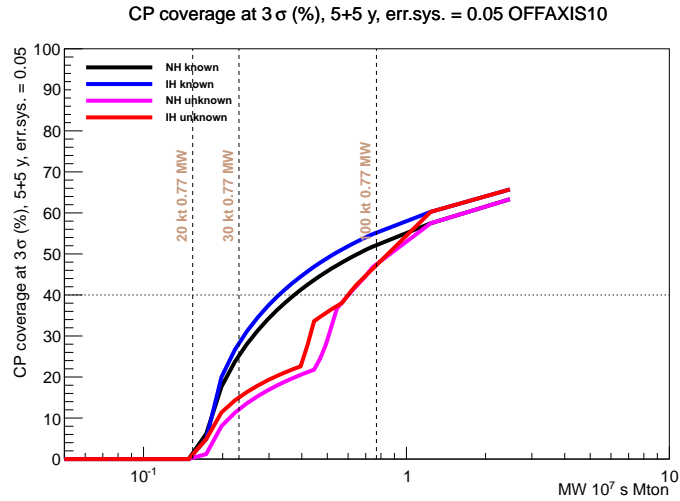


Figure 8: CP coverage at 3σ for 5 years of ν and 5 years of $\bar{\nu}$ running with the off-axis 10 km configuration, a 400 GeV proton driver and a systematic error on flux normalization of 5%. We consider normal and inverted hierarchy assuming this information to be either available or not (color codes).

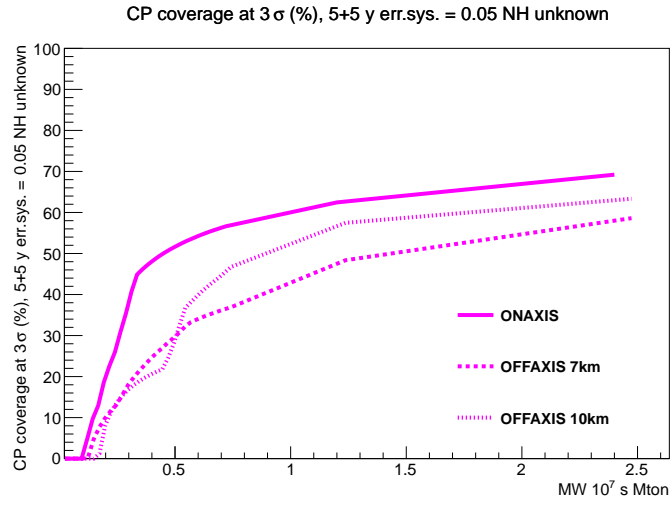


Figure 9: Comparison of the CP coverage at 3σ for 5 years of ν and 5 years of $\bar{\nu}$ running with the on-axis 50 GeV configuration, off-axis 7 and 10 km configuration and 400 GeV proton driver, and a systematic error on flux normalization of 5 %. Here we only consider normal hierarchy, which is assumed to be unknown.

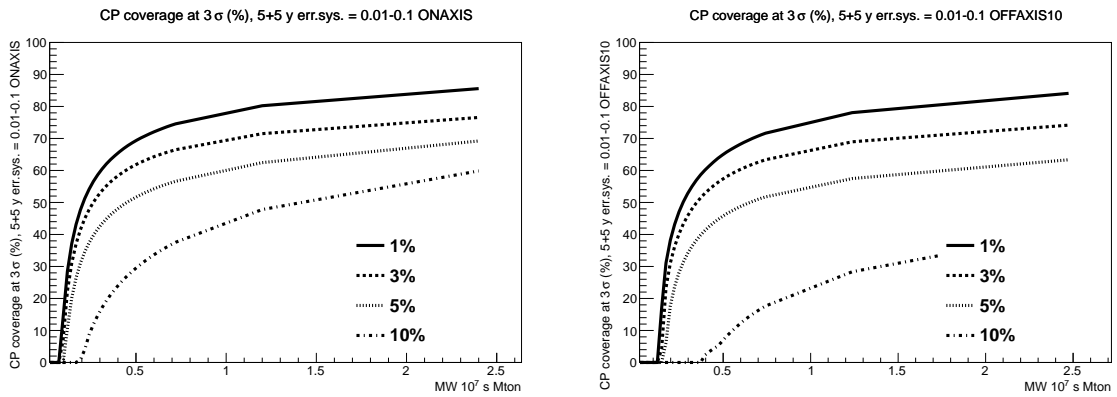


Figure 10: Effect of systematics on the CP coverage for the on axis (left) and off-axis 10 km (right) configurations.

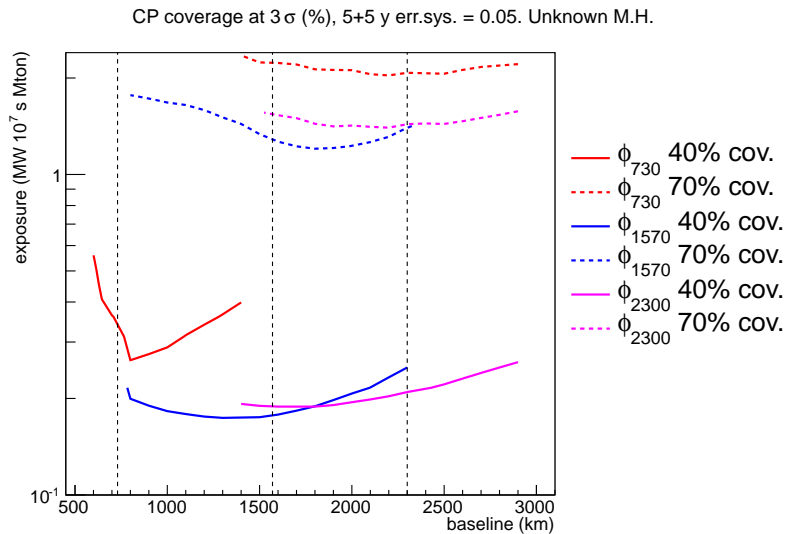


Figure 11: Exposure needed to reach 40% (solid line) and 70% (dashed line) CP coverage as a function of the baseline. The red, blue and purple contours are drawn considering the optimal beamline (see Sec. 3) for a 730, 1570 and 2300 km baseline, respectively.

In Fig. 11 we show the 70% and 40% CP coverage contours as a function of baseline and exposure for three different beamline configurations. The configurations are labeled Φ_{730} , Φ_{1570} and Φ_{2300} : they correspond to beam parameters optimized (see Sec. 3) for $L = 730, 1570, 2300$ km, respectively. In addition, Fig. 12 shows the 3σ CP coverage for the CERN-to-Phyäsalmi (2290 km) facility based on a dedicated 50 GeV proton driver. The same facility without the dedicated proton driver, i.e. leveraging the existing SPS complex has a CP coverage described in Fig. 13. As far as mass hierarchy is known in advance, medium baselines from 700 to 2300 km exhibit similar performance to establish CP violation in the leptonic sector. In fact, larger baselines are slightly favoured due to the broader neutrino energy range and, hence, due to the increase of spectral information. Spectral information also reduce the dependence of the coverage on the knowledge of the overall flux normalization and slightly relieve the deterioration of sensitivity due to systematics [49, 50].

In this framework, the optimal baseline is somehow in between LNGS and Phyäsalmi, i.e. at $L \simeq 1800$ km (Fig. 11). At $L \simeq 2000$ km the CP reach is independent of the mass hierarchy because the sign of Δm_{23}^2 can be established during data taking for all values of δ . This is not the case for facilities at $L \simeq 730$ km, where the mass hierarchy sensitivity hardly exceeds the one of the NOVA experiment [51] (see Fig. 14). Here, the mass hierarchy coverage is defined as the fraction of possible (true) values of the CP phase δ where the wrong hierarchy hypothesis is disfavoured at 3σ level.

5 Conclusions

The remarkable size of θ_{13} makes Superbeams the most straightforward choice for precision physics in the neutrino sector. While the determination of the mass hierarchy seems at reach for the next generation of facilities, the study of CP violation remains a major experimental challenge. Superbeams at medium baselines offer a clean environment to study CPV, provided that the mass hierarchy is known by the time of running or the sign ambiguity is resolved employing spectral information. However, major technological efforts are required to attain appropriate neutrino fluxes. In this paper we reconsidered medium baseline superbeams with special emphasis on CERN-based facilities, which have been re-optimized simulating the beam-

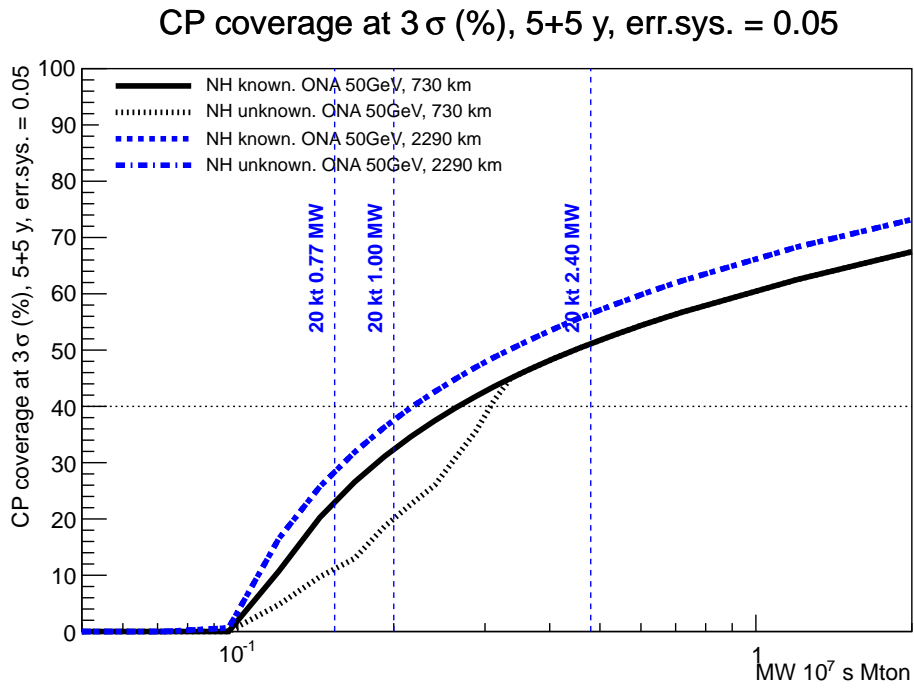


Figure 12: CP coverage for the facilities based on the 50 GeV proton driver (see text for details).

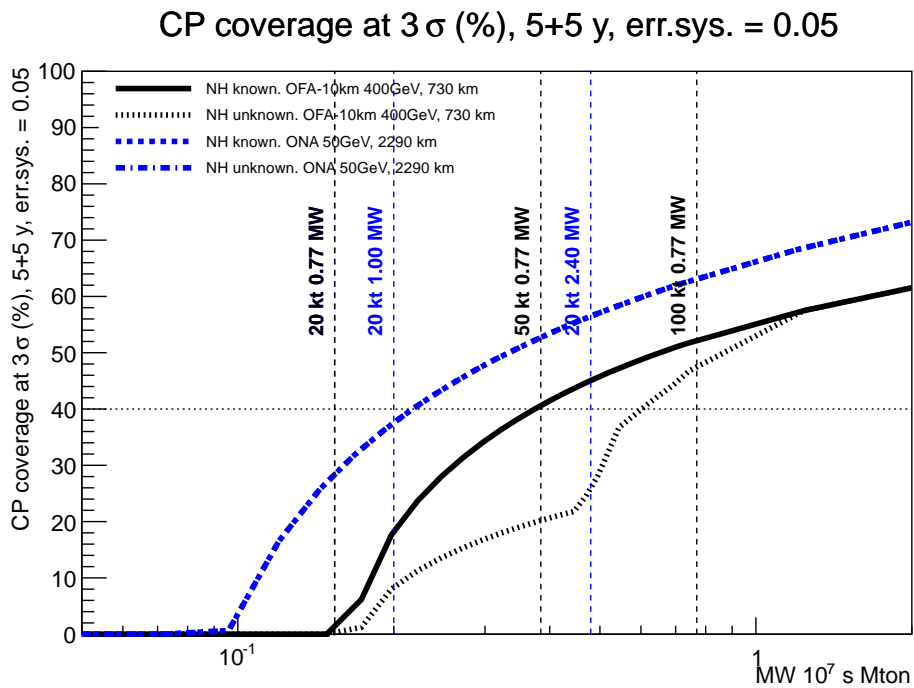


Figure 13: CP coverage for the facilities based on SPS (400 GeV proton driver) 10 km off-axis, and on a dedicate driver (50 GeV) at L=2290 km.

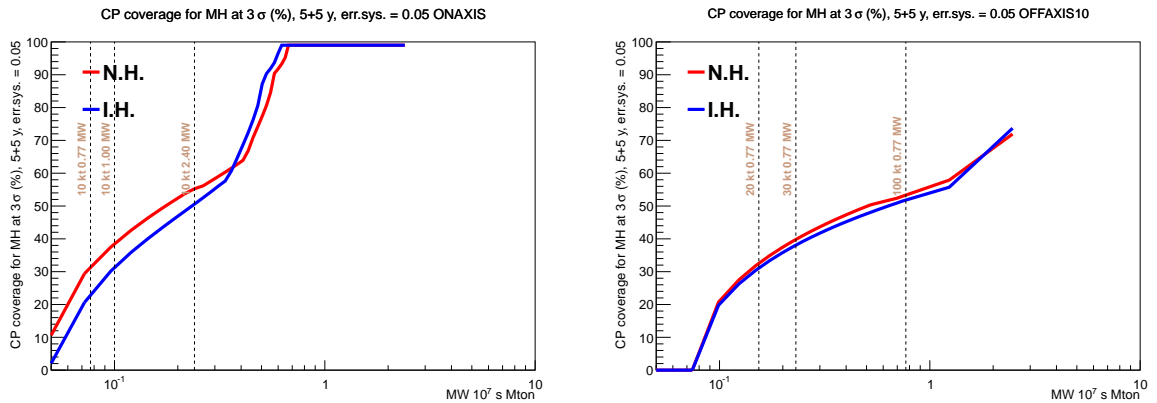


Figure 14: Mass hierarchy coverage for the 50 GeV on-axis option (left) and the 400 GeV 10 km off-axis option.

line from target to the decay tunnel. Facilities that are based on the CERN-SPS and exploit the CNGS beamline (off-axis 10 km) reach a modest CPV coverage in any realistic configuration: at most 52% (48%) with a 100 kton detector in a new shallow laboratory, assuming the mass hierarchy to be (not) known. Hence, a dedicated high-power driver is mandatory for CPV studies. Similar considerations hold at longer baselines. Here we considered specifically the CERN-to-Phyäsalmi distance, corresponding to 2290 km, and a new on-axis neutrino beam from CERN. For a detector mass of 100 kton the CPV coverage is 62% and drops to 28% if the LAr mass is lowered to 20 kton. On the other hand, at large baselines, the size of matter effects allows for a determination of the mass hierarchy for any value of δ . Hence, the facility does not suffer from the sign ambiguity even if the sign of Δm_{23}^2 is unknown a priori. The optimal facility to address CPV is an on-axis configuration (see Figs. 9,10) with a dedicated high power proton driver. A 100 kton detector hosted in a new underground facility at $L \simeq 730$ km could reach a CPV coverage of $\sim 70\%$, fully dominated by systematic uncertainties: 70% coverage for an overall systematic uncertainty of 5% and 86% coverage if the systematics can be brought down to the (currently unrealistic) value of 1%. Hence, in way similar to what happened with reactor experiments from Chooz to Daya Bay, novel techniques must be developed to lower systematics at the percent level in order to overcome the $O(70\%)$ coverage limit.

Acknowledgments

We wish to express our gratitude to P. Coloma, E. Fernandez-Martinez, F. Ferroni, A. Masiero, A. Mereaglia, A. Rubbia, C. Rubbia and L. Votano for useful information and suggestions.

References

- [1] Y. Itow *et al.* [The T2K Collaboration], “The JHF-Kamioka neutrino project,” arXiv:hep-ex/0106019.
- [2] F. Ardellier *et al.* [Double Chooz Collaboration], “Double Chooz: A search for the neutrino mixing angle $\theta(13)$,” arXiv:hep-ex/0606025.
- [3] X. Guo *et al.* [Daya-Bay Collaboration], “A precision measurement of the neutrino mixing angle $\theta(13)$ using reactor antineutrinos at Daya Bay,” arXiv:hep-ex/0701029.
- [4] S. B. Kim [RENO Collaboration], “RENO: Reactor experiment for neutrino oscillation at Yonggwang,” AIP Conf. Proc. **981** (2008) 205 [J. Phys. Conf. Ser. **120** (2008) 052025].
- [5] F. P. An *et al.* [DAYA-BAY Collaboration], Phys. Rev. Lett. **108** (2012) 171803

- [6] J. K. Ahn *et al.* [RENO Collaboration], Phys. Rev. Lett. **108** (2012) 191802
- [7] M. Ishitsuka for the Double Chooz Collaboration, Talk at Neutrino 2012, Kyoto, 6-9 June 2012, available at <http://neu2012.kek.jp>.
- [8] K. Abe *et al.* [T2K Collaboration], Phys. Rev. Lett. **107** (2011) 041801; K. Sakashita for the T2K Collaboration, Talk at ICHEP 2012, Melbourne, 4-11 July 2012, available at www.ichep2012.com.au
- [9] M. Apollonio *et al.* [CHOOZ Collaboration], Eur. Phys. J. C **27** (2003) 331.
- [10] F. Boehm *et al.*, Phys. Rev. D **64** (2001) 112001.
- [11] G. Altarelli and F. Feruglio, New J. Phys. **6** (2004) 106
- [12] M. Mezzetto and T. Schwetz, J. Phys. G G **37** (2010) 103001
- [13] A. Bandyopadhyay *et al.* [ISS Physics Working Group Collaboration], Rept. Prog. Phys. **72** (2009) 106201
- [14] R. Battiston, M. Mezzetto, P. Migliozzi and F. Terranova, Riv. Nuovo Cim. **033** (2010) 313
- [15] G. L. Fogli, E. Lisi, A. Marrone, D. Montanino, A. Palazzo and A. M. Rotunno, Phys. Rev. D **86** (2012) 013012
- [16] P. Huber, M. Lindner, M. Rolinec, T. Schwetz and W. Winter, Phys. Rev. D **70** (2004) 073014
- [17] V. Barger, P. Huber, D. Marfatia and W. Winter, Phys. Rev. D **76** (2007) 053005
- [18] P. Huber, M. Lindner, T. Schwetz and W. Winter, JHEP **0911** (2009) 044
- [19] P. Coloma and E. Fernandez-Martinez, JHEP **1204** (2012) 089
- [20] P. Coloma, A. Donini, E. Fernandez-Martinez and P. Hernandez, JHEP **1206** (2012) 073
- [21] P. Coloma, E. Fernandez-Martinez and L. Labarga, JHEP **1211** (2012) 069
- [22] V. Barger, M. Dierckxsens, M. Diwan, P. Huber, C. Lewis, D. Marfatia and B. Viren, Phys. Rev. D **74** (2006) 073004
- [23] T. Akiri *et al.* [LBNE Collaboration], “The 2010 Interim Report of the Long-Baseline Neutrino Experiment Collaboration Physics Working Groups,” arXiv:1110.6249 [hep-ex]
- [24] B. Baibussinov, M. Baldo Ceolin, G. Battistoni, P. Benetti, A. Borio, E. Calligarich, M. Cambiaghi and F. Cavanna *et al.*, Astropart. Phys. **29** (2008) 174
- [25] D. Autiero, J. Aysto, A. Badertscher, L. B. Bezrukov, J. Bouchez, A. Bueno, J. Busto and J. -E. Campagne *et al.*, JCAP **0711** (2007) 011
- [26] A. Rubbia, J. Phys. Conf. Ser. **171** (2009) 012020
- [27] D. Angus *et al.* [LAGUNA Collaboration], “The LAGUNA design study- towards giant liquid based underground detectors for neutrino physics and astrophysics and proton decay searches,” arXiv:1001.0077 [physics.ins-det]
- [28] A. Rubbia [LAGUNA Collaboration], Acta Phys. Polon. B **41** (2010) 1727
- [29] S. K. Agarwala, T. Li and A. Rubbia, JHEP **1205** (2012) 154
- [30] A. Rubbia, Talk at Neutrino 2012, Kyoto, 6-9 June 2012, available at <http://neu2012.kek.jp>
- [31] M. Freund, Phys. Rev. **D64** (2001) 053003. See also K. Asano and H. Minakata, JHEP **1106** (2011) 022
- [32] L. Votano, Talk at ν TURN2012, LNGS, 8-10 May 2012, available at <http://nuturn2012.lngs.infn.it/>.
- [33] S. Amerio *et al.* [ICARUS Collaboration], Nucl. Instrum. Meth. A **527** (2004) 329.
- [34] C. Rubbia, M. Antonello, P. Aprili, B. Baibussinov, M. B. Ceolin, L. Barze, P. Benetti and E. Calligarich *et al.*, JINST **6** (2011) P07011

- [35] F. Arneodo *et al.* [ICARUS Collaboration], “The ICARUS experiment: A Second generation proton decay experiment and neutrino observatory at the Gran Sasso Laboratory,” hep-ex/0103008; P. Aprili *et al.* [ICARUS Collaboration], “The ICARUS experiment: A second-generation proton decay experiment and neutrino observatory at the Gran Sasso laboratory. Cloning of T600 modules to reach the design sensitive mass,” CERN-SPSC-2002-027
- [36] C. Rubbia, Talk at ν TURN2012, LNGS, 8-10 May 2012, available at <http://nuturn2012.lngs.infn.it/>
- [37] A. Longhin. “Optimization of neutrino beams for underground sites in Europe,” arXiv:1206.4294v1
- [38] S. Agostinelli *et al.* [GEANT4 Collaboration], Nucl. Instrum. Meth. A **506** (2003) 250; J. Allison *et al.*, [GEANT4 Collaboration], IEEE Transactions on Nuclear Science **53** (2006) 270.
- [39] P. Huber, M. Lindner and W. Winter, Comput. Phys. Commun. **167** (2005) 195
- [40] P. Huber, J. Kopp, M. Lindner, M. Rolinec and W. Winter, Comput. Phys. Commun. **177** (2007) 432
- [41] M. Bonesini, A. Marchionni, F. Pietropaolo and T. Tabarelli de Fatis, Eur. Phys. J. C **20** (2001) 13
- [42] A. Meregaglia and A. Rubbia, JHEP **0611** (2006) 032
- [43] A. Ankowski *et al.* [ICARUS Collaboration], Acta Phys. Polon. B **41** (2010) 103
- [44] C. Andreopoulos, A. Bell, D. Bhattacharya, F. Cavanna, J. Dobson, S. Dytman, H. Gallagher and P. Guzowski *et al.*, Nucl. Instrum. Meth. A **614** (2010) 87
- [45] P. Huber, M. Lindner and W. Winter, Nucl. Phys. B **645** (2002) 3
- [46] H. Minakata and H. Nunokawa, JHEP **0110** (2001) 001
- [47] V. Barger, D. Marfatia and K. Whisnant, Phys. Rev. D **65** (2002) 073023
- [48] P. Huber, M. Mezzetto and T. Schwetz, JHEP **0803** (2008) 021
- [49] P. Coloma, P. Huber, J. Kopp and W. Winter, “Systematic uncertainties in long-baseline neutrino oscillations for large θ_{13} ,” arXiv:1209.5973 [hep-ph]
- [50] P. Coloma, T. Li and S. Pascoli, “A Comparative Study of Long-Baseline Superbeams within LAGUNA for large θ_{13} ,” arXiv:1206.4038 [hep-ph]
- [51] D. S. Ayres *et al.* [NOvA Collaboration], “NOvA proposal to build a 30-kiloton off-axis detector to study neutrino oscillations in the Fermilab NuMI beamline,” arXiv:hep-ex/0503053; D. S. Ayres *et al.*, The NOvA Technical Design Report, FERMILAB-DESIGN-2007-01 (2007)